J Mol Model (2014) 20:2535
DOI 10.1007/s00894-014-2535-7

ORIGINAL PAPER

Optoelectronic and nonlinear optical properties of triarylamine helicenes: a DFT study

Nasarul Islam · Altaf Hussain Pandith

Received: 27 April 2014 / Accepted: 17 November 2014 / Published online: 11 December 2014

Abstract This work involved the design of a new series of triarylaminehelicenes (TAH) with significant hole transport capacity and enhanced nonlinear optical response. The geometries, electronic properties and nonlinear response of TAH derivatives were studied using density functional theory at the B3PW91/6-311++G (2d, 2p) level. Charge transfer and nonlinear optical response were analyzed and correlated with modifications in geometry and energy levels. Calculations indicated that trivial changes in the torsional angle occur in TAH derivatives with electron-donating substituents as compared to those with electron-withdrawing substituents, resulting in lower reorganization energies for TAH derivatives **2**–**6**. TAH derivatives with an $–N(CH_3)_2$ group have the greatest highest occupied molecular orbital (HOMO) level, and thus the least ionization potential, indicating significant hole transfer efficiency as compared to unsubstituted TAH. A decrease in the HOMO–LUMO gap occurs upon substitution with electron-releasing groups, whereas there is an increase in the case of $–NO_2$, –COOH, and –CN TAH derivatives. Topological analysis of the HOMOs of the neutral molecules revealed that these orbitals are concentrated mainly in the helicene backbone, with an important contribution from fused phenyl rings, nitrogen atoms and carbonyl groups. However, the lowest unoccupied molecular orbitals (LUMO) are invariably constituted by fused phenyl rings without any contribution from the central nitrogen atom. Studying the effect of substitution on the nonlinear optical response of TAH derivatives, the calculated polarizability and hyperpolarizability at B3PW91/6-311++G (2d,2p) level of theory exhibited a prominent improvement as compared to unsubstituted TAH. Both electron-donating groups and electron-withdrawing groups result in a red shift in the electronic absorption bands of the substitution derivatives, in particular those with $–N(CH_3)_2$ and $–NH_2$ groups.

Keywords Reorganization energy · Hammett parameter · Conjugation · Bond length alternation · Hyperpolarizability

Introduction

Recently, there has been increasing demand for computational chemistry in the design, modeling and screening of novel electronic and nonlinear optical responses of organic materials [1, 2]. Organic semiconducting materials based on π-conjugated chemical structures have been synthesized and studied over many decades due to their potential applications in organic electronic devices like organic light emitting diodes (OLEDs) and photovoltaic cells [3–8]. In this context, the synthesis and extensive investigation of the electronic properties of bridged triarylaminehelicenes (TAH) have attracted much attention in recent years [9–14]. The emergence of this class of electro-active helicenes has opened up the possibility of developing new electro-optics, photonics, display devices and ultra-fast optical data processing devices[15–20]. These systems are comprised of ortho-fused aromatic rings and possess a rigid helical framework. Single-crystal X-ray diffraction of these helicenes shows that their helical twist is sterically driven by the increasing overlap of the terminal aryl rings. These materials find applications in OLEDs, where they increase device performance substantially if placed as a hole transport layer (HTL) between the anode and the luminescent layer. A distinguishing characteristic of TAH potential hole transport materials is that these can reversibly form radical cations, i.e., they can accept and donate positive charges without decomposition, which makes them the material of

Electronic supplementary material The online version of this article (doi:10.1007/s00894-014-2535-7) contains supplementary material, which is available to authorized users.

N. Islam · A. H. Pandith (✉)
Department of Chemistry, University of Kashmir, Srinagar, Kashmir 190006, India
e-mail: altafpandit23@gmail.com

choice amongst many organic hole transport materials. The charge transport and conductance of these systems depend on the extent of their helicity [21]. Therefore, these molecular systems can be used as a model for understanding the effect of helicity on bulk electronic properties [22].

The band gap of bridged TAH systems is flexible and depends on the radius of the helix and the width of the helical ribbon and can, therefore, be tuned into forms having useful semiconducting or metallic properties. The tuneable energy gaps of these molecules make them promising candidates for applications in solar cells and OLEDs. In this respect, these systems can be compared to graphene [23–26], its low dimensional forms like 1-D nanotubes, 1-D nano ribbons, 0-D graphene quantum dots (GQDs) [27–30], and its inorganic analogues like boron-nitride (BN), transition metal dichalcogenides, etc. [31–33]. There is growing interest in incorporating graphene, its functionalized forms and its low dimensional sister compounds, into organic photovoltaics, particularly as conducting electrodes [34, 35] and as hole transport layers [36, 37]. The band-gap and other electronic properties of these low dimensional graphene forms depends on several factors such as their size and shapes (GQDs), ribbon widths (nano-ribbons), passivation and edge geometry [38–40]. Recently, many works have demonstrated convincingly, both theoretically and experimentally, that fine tuning of the band gaps [highest occupied molecular orbital (HOMO)–lowest unoccupied molecular orbital (LUMO) gaps] of graphene, its low dimensional analogues like carbon nano-tubes, GQDs, and their inorganic counterparts like boron nitride quantum dots (BNQDs) can be engineered effectively through charge transfer (CT) mechanisms by doping electron donor/acceptor molecules on the graphitic substrates. Thus, for efficient OLED applications, the simplest possible ways of fine-tuning the HOMO–LUMO gaps of bridged TAHs could include molecular CT interactions through substitution/ functionlization based on the electron donating/accepting nature of the substituents.

In organic systems, CT is explained by hopping theory [41] and band theory [42]. In the hopping model, CT occurs between small coupled neighboring molecules, and the rate constant of the CT is an activation-barrier controlled process. However, in band theory, CT is considered an activationless process occurring via bands formed by overlapping of molecular orbitals between neighboring molecules. As per the Marcus electron–transfer theory [43, 44], the rate of hole or electron-transfer k_{et} (by hopping) is given by following equation:

$$k_{et} = \left(4\pi^2/h\right) H_{ab}^2 \left(4\pi\lambda_{+/-}\, T\right)^{-\frac{1}{2}} \exp\left(-\lambda_{+/-}/4kT\right) \quad (1)$$

Here, $\lambda_{+/-}$ is reorganization energy and H_{ab} is the CT integral. Several theoretical studies of charge transport properties of OLED materials suggest that both the reorganization energies and CT integrals are important parameters in electron/hole transport process [45–48]. According to Eq. 1, CT processes with lower λ+values should proceed with higher rate constants. The intramolecular reorganization energy (λ+) for self-exchange consists of two terms corresponding to the geometry relaxation energies upon going from the neutral-state geometry to the charged-state geometry and vice versa [46–49].

$$\lambda_{+/-} = \lambda_1 + \lambda_2 \quad (2)$$

$\lambda_{+/-}$ is an intramolecular property in nature and can be evaluated by quantum chemistry calculations. However, ΔH_{ab} can also be calculated by employing Koopmans' theorem in conjunction with the Hartree-Fock (HF) model. The direct coupling scheme for analogous molecules shows a rather narrow range of values for ΔHab [50, 51]. Therefore, we assume that the relative CT properties of TAH derivatives can safely be accounted for on the basis of their respective reorganization energies. The reorganization energies of TAHs were calculated from Scheme 1, where λ_1 is the stabilization energy of the geometry relaxation of the molecule upon formation of the corresponding cation radical. The reorganization energy λ_2 is the energy difference between the vertical electron affinity and the adiabatic electron affinity of the cation radical. The total reorganization energy λ_+ is the arithmetic sum of the two reorganization energies, λ_1 and λ_2.

The conjugated pathways arising from the helix framework in helicenes allow helical motion of the polarizable electrons, which give rise to their second-order nonlinear optical (NLO) response. It has been found that, even in the absence of electron donor or acceptor groups, a sizable second-order NLO response at the molecular level exists [52–57]. According to Verbiest et al. [21], chirality of the helicenes is responsible for their second order NLO response. The transition dipole moment from the ground state to the optically active

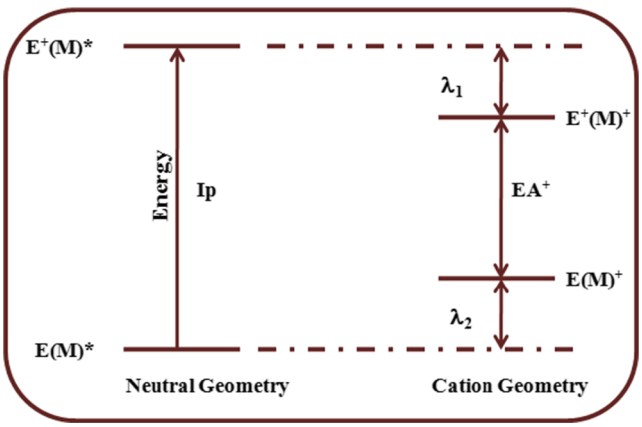

Scheme 1 Calculation details of the reorganization energy for electron transport. λ_1 Reorganization energy of cationic-radical, λ_2 reorganization energy of a neutral molecule

state increases due to CT, thereby controlling the NLO response of the system [55]. Spassova et al. [58] reported a theoretical investigation on the electronic circular dichroism spectra of bridged TAHs. In our earlier work, we reported on the conformational analysis and vibrational circular dichroism of TAH and its camphanate derivative [59].

Quantum computation offers an inexpensive way to evaluate the NLO properties of materials using theoretical calculations. The characteristic NLO properties of a variety of microscopic systems, including molecules and clusters, have been studied extensively in terms of polarizability (α) and hyperpolarizability (β) by using quantum chemical methods. We calculated the electric dipole moment, the isotropic polarizability and the first hyperpolarizability, in order to understand the microscopic NLO mechanisms of TAH derivatives. Polarizability is a measure of the change in a molecule's electron distribution in response to an applied electric field, which can also be induced by electric interactions with solvents or ionic reagents. On the other hand, the permanent electric dipole moment is a measure of the charge density in a molecule, its magnitude and direction being sensitive to molecular size and shape of the molecule. The microscopic polarizability (P) induced in an isolated molecular under the applied electric field (E) of an incident electromagnetic wave is expressed by the equation

$$\boldsymbol{P} = \boldsymbol{\alpha_E} + \boldsymbol{\beta_E} \tag{3}$$

Where α and β refer to the polarizability and first hyperpolarizability, respectively. In order to calculate the polarizability and hyperpolarizabilities, different derivatives of energy or dipole moment were related to various coefficients of power series expansions using derivative methods. The total static dipole moment (μ), average linear polarizability (α) and first-order hyperpolarizability (β) using the x, y, z components of the compound from Gaussian 03 W [60] output were calculated by Eqs. 4–6 [61–77].

$$\boldsymbol{\mu} = \left(\boldsymbol{\mu_x^2} + \boldsymbol{\mu_y^2} + \boldsymbol{\mu_z^2}\right)^{1/2} \tag{4}$$

$$\boldsymbol{\alpha} = {}^{1}/_{3}\left(\boldsymbol{\alpha_{xx}} + \boldsymbol{\alpha_{yy}} + \boldsymbol{\alpha_{zz}}\right) \tag{5}$$

$$\boldsymbol{\beta} = [(\boldsymbol{\beta_{xxx}} + \boldsymbol{\beta_{xyy}} + \boldsymbol{\beta_{xzz}})^2 + (\boldsymbol{\beta_{yyy}} + \boldsymbol{\beta_{yzz}} + \boldsymbol{\beta_{yxx}})^2 + (\boldsymbol{\beta_{zzz}} + \boldsymbol{\beta_{zxy}} + \boldsymbol{\beta_{zyy}})^2]^{1/2} \tag{6}$$

A good understanding of electronic properties such as reorganization energy, HOMO–LUMO energy gap and ionization potential, etc., is a key factor in the design of new and novel hole transport materials and materials with NLO properties. This work encompasses a theoretical study of the CT and NLO response of several derivatives of TAH using quantum chemical computations and an investigation of the substitution effect on the molecular framework of TAH, in terms of change in their energy levels, nonlinear response and hole transport behavior. The substituents were chosen in order to cover functional groups with a wide range of Hammett parameters ranging from $-N(CH_3)_2$ to $-NO_2$.

Theoretical calculations

For all calculations, we employed density functional theory (DFT), using Becke's three parameter (B3PW91) [65] exchange-correlation functional and the 6-311++ G(2d,2p) [66, 67] basis set as implemented in Gaussian 03 [60]. Geometry optimthe gas phase and were characterized as minima with zero imaginary frequencies. The neutral and cation molecules were treated as closed-shell systems, while for the radical cation open-shell system optimizations were carried out using a spin-unrestricted wave function (UB3PW91) procedure. The excited state characteristics (exCitation energies, transition dipole integral, rotatory strengths) were determined using adiabatic approximation using a time-dependent density functional approach (TDDFT) [68] employing the B3PW91fuctional and 6-311++ G(2d,2p) basis set. The computational cost of TDDFT is roughly comparable to single-excitation theories based on a HF ground state, such as single-excitation configuration interaction (CIS); however, numerical applications reported so far indicate that TDDFT employing current exchange-correlation functional performs significantly better than HF-based single-excitation theories for the low-lying valence excited states of both closed shell and open-shell molecules [69–72].

Results and discussion

Geometry

Starting from the optimal structure of TAH where X=H, [TAH (**1**)], various substitution-based TAH derivatives were built by replacing **X** with the following electron-donating [$-N(CH_3)_2$, $-NH_2$, $-C(CH_3)$, $-C_2H_5$ and $-CH_3$] and electron-withdrawing (–F, –Cl, –Br, –COOH, –CN and $-NO_2$) groups. DFT calculations were used for geometry optimizations of derivative monomers with the donor (2–6) and acceptor (7–12) substituents given in Scheme 2. The substituents were chosen in a manner to cover the possible wide range of the

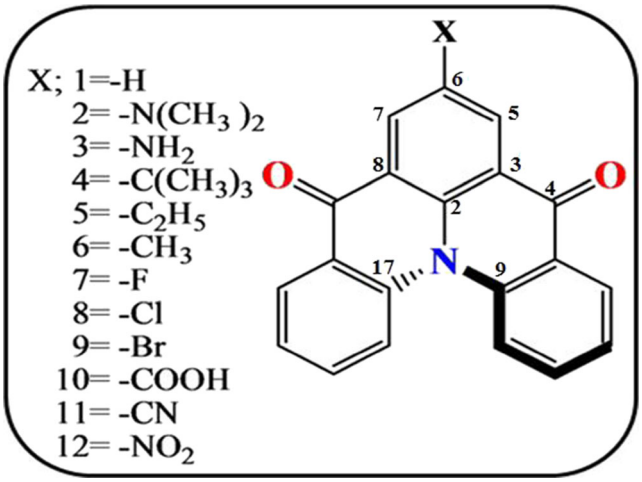

Scheme 2 Sketch of triarylaminehelicene (TAH) derivatives in this study using DFT at B3PW91/6-311G (2d, 2p) ++ level of theory

Hammett parameter (σ). The Hammett parameter is defined as measure of electron density increase or decrease when functional groups are attached to chemical system [73]. In this work, we carried out comparative correlation studies of the substitution effect on helicene monomers and their opto-electronic properties by employing theoretically calculated parameters of interest like reorganization energy, optical band gap, polarizability and hyperpolarizability in relation to geometrical parameters, Hammett parameters and bond length alternation (BLA), followed by interpretation of the observed relationships. The optimized geometrical structures of the studied systems **1**–**12** are shown in Fig. S1 (supporting information) and some selected bond lengths, bond angles and interplanar angles of TAH are listed in Table S1 (supporting information). A comparison of calculated geometrical parameters with corresponding experimental values [13] show reasonable agreement between the two, indicating that the adopted basis functional and basis set were appropriate for the systems under investigation. The slight deviations observed may be attributed to the fact that the theoretical calculations were performed for monomeric molecules in gaseous phase and experimental values were obtained from the crystalline solid phase. The geometry of TAH (**1**) reveals the presence of three aryl rings linked through two bridged carbonyl groups and a planar central nitrogen atom. In the optimized gas phase geometries, the terminal rings are out of plane with an interplanar angle of 46.19°. In the case of the parent molecule [TAH (**1**)], of the three N–C bonds, the N–C_2 bond (1.399Å) is shorter compared to the N–C_9 and N–C_{17} (1.419Å) bonds. To account for the substitution effect on structural parameters of TAH, we carried out a comparative study of the change in N–C_2, N–C_9 and N–C_{17} bond lengths, C_2–N–C_{17} and C_{17}–N–C_9 bond angles and C_{18}–C_{17}–C_9–C_{10}interplanar angles upon substitution with selected electron-releasing and electron-withdrawing groups. From Table 1, we observe that the N–C_2 bond length increases with electron-donating substituent and shortens with electron-withdrawing substituents as compared to unsubstituted TAH(**1**), while N–C_9 and N–C_{17} bond lengths shorten with electron-donating substituents and elongate with electron-withdrawing groups. Expansion of the N–C_2 bond in substituted TAHs **2**–**6** results from increased repulsion between the enhanced electron density due to electron-donating groups and the lone pair of nitrogen, whereas contraction of the N–C_2 bond in substituted TAHs **7**–**12** is result of increased attraction on the electron cloud due to scarcity caused by electron-withdrawing groups.

The extent of planarity of the carbon atoms around nitrogen atom is reflected in the BLA values of TAH derivatives. In this work, we calculated a local BLA associated with N–C_2, C_2=C_3 and C_3–C_5 bond lengths according to the definition of Fu et al. [74] given in Eq. 7:

$$\mathbf{BLA} = \frac{\mathbf{d}(\mathbf{N}-\mathbf{C}_2) + \mathbf{d}\,(\mathbf{C}_3-\mathbf{C}_5)}{2} - \mathbf{d}(\mathbf{C}_2 = \mathbf{C}_3) \qquad (7)$$

The change in bond length of TAH derivatives show the increased double bond character of the central single bond in the case of TAH derivatives with electron-donating groups, indicating an increase in the degree of conjugation as compared to TAH derivatives with electron-withdrawing substituents. The increase in electron density due to electron-donating groups on TAH(**1**) is in the order of **6**<**5**<**4**<**3**<**2** and the BLA values increase from 0.369 (**2**) <0.371(**3**) <0.375(**4**)<0.381(**5**) <0.382(**6**) <0.384 (**1**), indicating that the degree of conjugation increases upon substitution with electron-donating groups. However, the correlation between BLA and the electron-withdrawing capacity of substituents is inconsistent. TAH(**11**) and TAH(**12**) have maximum electron-withdrawing capacity, with highest BLA values of 0.385 and 0.389, respectively, but in the case of **7**, **8** and **9**, electron-withdrawing capacity decreases in the order **7**>**8**>**9**, but the BLA values do not differ much [0.385(**7**)<0.386(**8**)= 0.386(**9**)].

In order to study the hole transport properties of TAH systems, we optimized the cationic geometry (i.e., the neutral molecule in the absence of an electron) to understand the effects of charge extraction on molecular conformational stability and electron release in these molecules. A modification of structural parameters (bond lengths and interplanar angle) in the radical-cation with respect to neutral systems was observed. The interplanar angle of TAH (**1**) changed from 45.56° to 47.36°; however, the dihedral angles (CCNC and CCNC) between the terminal aryl ring showed a negligible change. The bond length of the C_2–N bond increased slightly from 1.400 to 1.429Å. The central moiety retains planarity, indicating that there is little affect on structural stability as the

Table 1 Geometrical parameters of triarylaminehelicene (TAH) derivatives in neutral and cationic states calculated at B3PW91/6-311G (2d, 2p)++ level of theory

Compound	C_{17}-N-C_9	Cationic	C_2-N	Cationic	C_{17}-N	Cationic	C_9-N	Cationic	C_{18}-C_{17}-C_9-C_{10}	
	Neutral		Neutral		Neutral		Neutral		Neutral	Cationic
1	122.73	121.60	1.400	1.429	1.420	1.413	1.420	1.427	45.56	47.36
2	123.12	122.78	1.404	1.417	1.416	1.414	1.417	1.418	44.28	45.30
3	123.02	122.68	1.403	1.418	1.416	1.414	1.416	1.418	44.55	45.74
4	122.90	122.53	1.402	1.418	1.418	1.415	1.418	1.422	45.10	46.29
5	122.86	122.30	1.401	1.417	1.419	1.413	1.419	1.425	45.14	46.61
6	122.88	122.43	1.401	1.417	1.419	1.413	1.419	1.425	45.16	46.57
7	122.83	123.60	1.400	1.417	1.419	1.411	1.419	1.428	45.67	47.17
8	122.84	123.78	1.398	1.415	1.420	1.411	1.420	1.429	45.68	47.20
9	122.83	123.82	1.398	1.417	1.420	1.412	1.420	1.428	45.63	47.17
10	122.61	123.85	1.395	1.415	1.422	1.411	1.422	1.433	46.01	47.76
12	122.65	123.91	1.394	1.414	1.422	1.410	1.423	1.435	46.01	47.77
13	122.56	123.84	1.392	1.418	1.424	1.411	1.424	1.438	46.20	47.97

optimized cationic geometries show only small structural changes compared to the natural molecules, which are close to triarylamine [75]. From plots of change in interplanar angle versus the Hammett parameter, we observed that, upon extraction of one negative charge from the system, the amplitude of structural modification from TAH derivatives increases with electron-donating substituents compared to TAH derivatives with electron-withdrawing substituents, signifying an apparent substitution effect on the TAH derivatives (see Fig. 1a). The plot of change in selected geometrical parameters versus σ indicate a correlation between the Hammett parameter and a change in geometrical parameters upon ionization (see Fig. 1b). It is pertinent to note that the substitution ranging from the group with the lowest Hammett value (dimethylamino) to the group with the highest Hammett value (nitro) affected the bond lengths, bond angles and interplanar angles of the TAH derivatives. The minimal change in interplanar angle due to electron-donating substituents was attributed to an increase in electron density, as it is easier to change a radical cation as compared to an electron-withdrawing group. Therefore, substitution with electron-releasing groups rendered the TAH structure more rigid during the process of ionization as compared to electron-withdrawing substituents. This structural stability upon ionization makes it feasible to use these systems for structural manipulation with the aim of fine tuning their properties to develop better hole transport systems.

Reorganization energy

We used the Gaussian 03 computational package [60] to calculate reorganization energies for hole transfer processes, using the Scheme 1 values given in Table 2. We found that, compared to the parent TAH (**1**), the value of λ_+ decreased for TAH derivatives with electron-releasing (**2**–**6**) and increased for TAH derivatives with electron withdrawing (**7**–**12**) substituents. The effect on reorganization energy was much more prominent in the case of electron-withdrawing substituents as compared to electron-donating substituents. In the case of electron-donating groups, the reorganization energy increased in the order of CH_3< $–C_2H_5$> $–C(CH_3)_3$> $–NH_2$> $–N(CH_3)_2$, and in the case of TAH derivatives with electron-withdrawing groups, the reorganization energy decreased in the order $–NO_2$> –CN> –COOH> –Br> –Cl= –F. From Fig. 2a, we observe a clear correlation between reorganization energies λ_+ and Hammett parameters: in the case of TAH derivatives with electron-donating substituents, λ_+ decreased with decrease in Hammett parameter values (R^2_{adj} =0.57). However, in the case of halogen derivatives there was no clear trend, except for THA derivatives **10**, **11** and **12**, wherein the reorganization energies achieved maximum values. All the derivatives with electron-donating groups show lower values for λ_+, which is related to the energy needed to undergo changes in the molecular structure after charge injection. Thus, on the basis of λ_+ values, the smallest impact due to charge injection was found in TAH (**2**), which is indicative of its improved efficiency as a hole transport material. In order to evaluate the defining parameters that effect reorganization energies of TAH derivatives, we correlated the reorganization energy values with the BLA and change in geometrical parameters upon release of one negative charge. The plot of reorganization energy against BLA (Fig. 2b) reveals that BLA values increased in order of **2**<**3**<**4**<**6**<**5** and the reorganization energy increased **2**>**3**>**4**>**6**>**5**. However, in the case of TAH derivatives with electron-withdrawing substituents, no clear dependence was seen, especially in the case of halogen

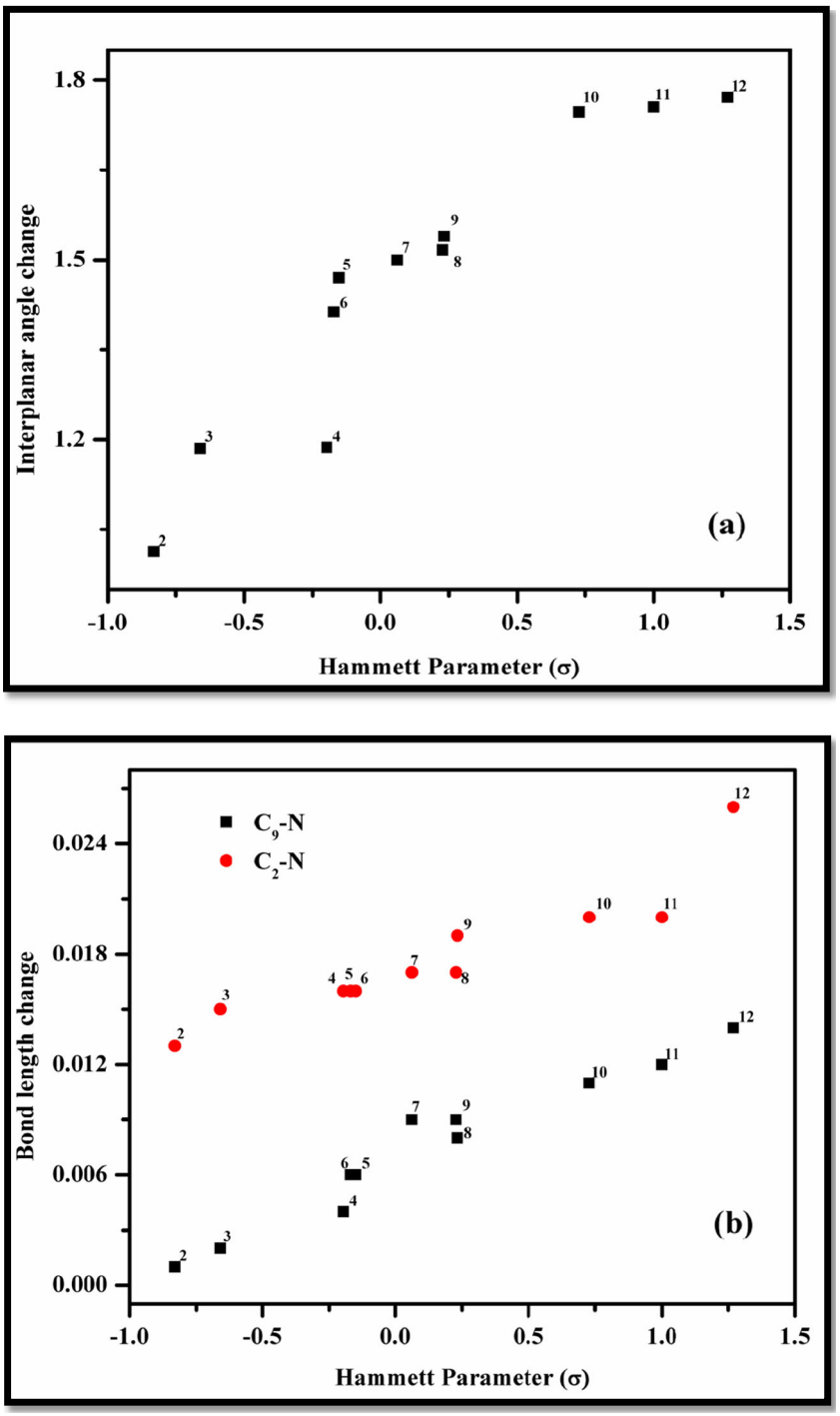

Fig. 1 Plot of geometrical change of **a** interplanar angle and **b** bond length versus the Hammett Parameter σ for the series of studied triarylaminehelicene (TAH) derivates

derivatives. The BLA values suggest increased conjugation and aromaticity in derivatives having higher electron-releasing substituents and minimum reorganization upon charge injection in such TAH derivatives.

We analyzed the correlation between reorganization energy values and changes in bond length, bond angle and interplanar angle. There was a significant correlation between reorganization energy (λ_+) and the change in geometrical parameters defined in terms of central interplanar angle (ΔC_{18} –C_{17} –C_9 –C_{10}) and bond length (C_2–N) and (C_9–N) (Fig. 3a,b). However, very poor correlation was found between reorganization energy and the<C_{17} –N–C_9 bond angle. In the case of TAH derivatives with electron-releasing substituents, small changes in geometrical parameters, particularly

Table 2 Reorganization energies of TAH derivatives for hole transport (and its λ_1 and λ_2 components) in eV calculated at DFT/ B3PW91/6-311G (2d, 2p) ++ level of theory and experimental Hammett parameter (σ)

Compound	λ_1	λ_2	λ_+	σ[a]
1	0.129	0.117	0.246	0
2	0.075	0.043	0.118	−0.83
3	0.082	0.055	0.137	−0.66
4	0.081	0.056	0.137	−0.2
5	0.081	0.056	0.137	−0.15
6	0.095	0.043	0.137	−0.17
7	0.082	0.056	0.137	0.062
8	0.087	0.050	0.137	0.227
9	0.087	0.051	0.137	0.232
10	0.097	0.041	0.138	0.45
11	0.099	0.044	0.143	0.66
12	0.122	0.106	0.227	0.778

[a] Ref. [60]

the interplanar angle, were consistent with small values of λ_+; the minimum value being observed for dimethyl amine (ΔC_{18} $-C_{17}$ $-C_9$ $-C_{10}$=1.01 , λ_+ =0.118). However, for TAH derivatives with electron-withdrawing groups, the trend show an irregular pattern, as the change in interplanar angles increased in the order –F< –Br< –Cl< –CN< –COOH< $-NO_2$ and reorganization energies follows the order –F= Cl< $-NO_2$< –COOH< –Br<CN. The rate of change in interplanar angle is slow in the case of **10**, **11** and **12** TAH derivatives, whereas their reorganization energies increase quickly. Thus, the strong electron-withdrawing substituents are responsible for large geometrical changes (interplanar angle change) as compared to weak electron-withdrawing or electron-donating substituents (e.g., halogens and alkyl groups cause only moderate geometry changes). Minimum changes in geometrical parameters, particular interplanar angles were observed in the case of TAH derivatives with strong electron-donating substituents [$-NH_2$< $-N(CH_3)_2$].

Electronic energy levels

Electronic energy levels were studied by employing B3PW91/6-311 ++ G (2d,2p) level of theory for isolated molecules. The energy levels (bands) allow for electrons and holes, and energy gaps between these bands govern the electronic properties of molecular systems. The difference between the energy of the lowest unoccupied molecular orbital (E_{LUMO}) and that of the highest occupied molecular orbital (E_{HOMO}), accessible to non-interacting electrons and holes represents the energy gap ($\Delta E_{LUMO–HOMO}$). In principle, among other things, the durability of OLEDs depends on the ionization potential of hole transport materials; the lower ionization potential, the higher durability of the device. It is clear from Table 3 that electron-releasing substituents [$-CH_3$> –C2H5< $-C(CH3)_3$< –NH2 < $-N(CH_3)_2$] increase the HOMO level of TAH derivatives with the increase in electron-releasing character, which results in a decrease of ionization potential of TAH derivatives. This trend is explained on the basis of an enhanced build up of the π-conjugation effect due to an increase in electron density originating from electron-rich substituents. However, there is a decrease in the HOMO–LUMO gap upon substitution with electron-releasing groups because the LUMO energies decrease as the electron-donating character of the substituents increase. This trend compares fairly well with the recently reported theoretical calculations on doping of electron donor molecules GQDs and BNQDs [76]. In the case of TAH derivatives with electron-withdrawing substituents, there is a decrease in the HOMO level of the TAH (as a result, there is an increase in ionization potential), which becomes more prominent with the increasing electron-withdrawing character of the substituents (–F> –Cl> $-NO_2$> –COOH> –Br> –CN). However, overall, the energy gap increases as the electron-withdrawing character of the substituent increases, because the LUMO energies increase, rather irregularly, with electron-withdrawing substituents. The ionization potential of the TAH derivatives increases with increasing electron-withdrawing character of the substituents, except in derivatives **8** and **9** (see Table 3). The overall magnitude of change in HOMO levels is bigger than those of LUMO levels, with both electron-releasing as well as electron-withdrawing groups as substituents. It was not possible to compare the calculated ionisation potential (IP) values of TAH derivatives with experimental values, as such data is not available in the literature; however, the plot of IP correlated quite well with σ, which points to an obvious substitution effect on energy levels in the studied systems (Fig. 4). The corresponding frontier molecular orbitals (FMOs) of all the TAH derivatives are shown in Fig. 5. Topological analysis of the HOMOs of the neutral molecules reveals that these orbitals are concentrated mainly in the helicene backbone with an important contribution of the fused phenyl rings, nitrogen atoms and of carbonyl groups. However, the LUMO orbitals are invariably constituted by the fused phenyl rings without any contribution from the central nitrogen atom. The molecular orbitals contributions are important in determining the charge-separated states of TAH derivatives. To create an efficient charge-separated state, the HOMO must be localized on the donor subunits and LUMO on the acceptor subunits [75]. In the TAH(**2**) derivative, the HOMO comprises both helical conjugate and substituent, which is indicative of enhanced CT efficiency. Moreover, the HOMOs of TAH derivatives with the dimethylamine and amine substituents are closer to the HOMOs of the anode (indium tin oxide) [77] as compared to the TAH(**1**) and TAH derivatives with electron-withdrawing substituents. Thus, TAH(**2**) and TAH(3) display high hole mobility on account

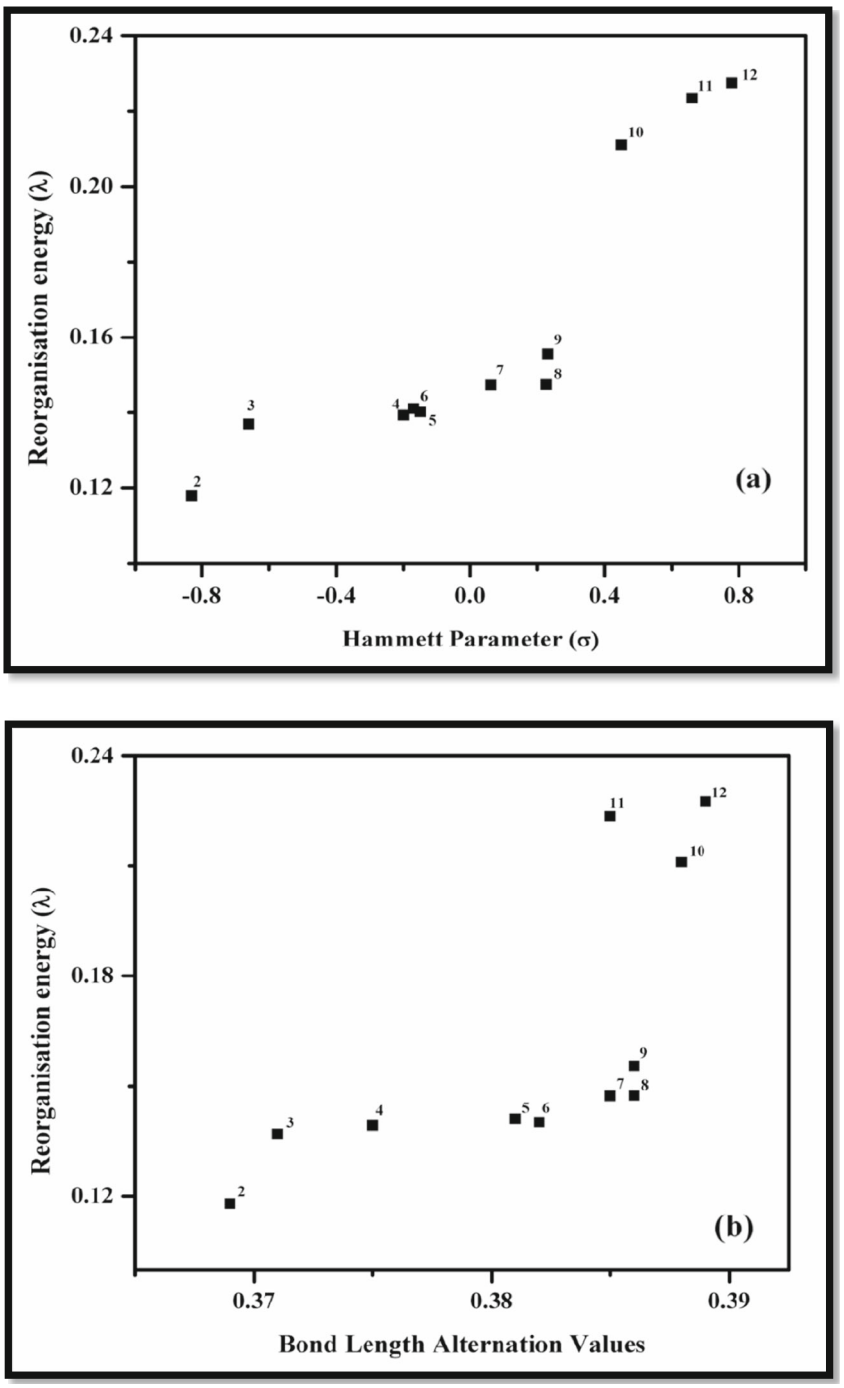

Fig. 2 Plot of reorganization energy with (**a**) Hammett parameter and (**b**) bond length alternation (BLA) values for a series of TAH derivatives

of lowering the barrier for electron ejection. The enhanced conjugative effect from the terminal groups can account for the possible red shift in λ_{max} of the electronic band for TAH derivative with electron-donating substituents with respect to unsubstituted TAH(**1**).Thus, by incorporating the electron-donating substituent to TAH (**1**), we were able to make the proper adjustment of the HOMO–LUMO gap of the hole-transport material (HTM) in order to facilitate easy oxidation, resulting in suitable IP, thereby allowing minimization of the barrier for electron extraction and ensuing the efficiency of CT by the derivative. Thus, a good understanding of the electronic properties, such as energy gap and frontier orbital levels, is a key factor in designing efficient HTM.

Nonlinear response

In this study, we calculated dipole moment, polarizabilities and hyperpolarizabilities for TAH derivatives using derivative method. Derivative method relates different derivatives of dipole moment or energy to various co-efficients of power series

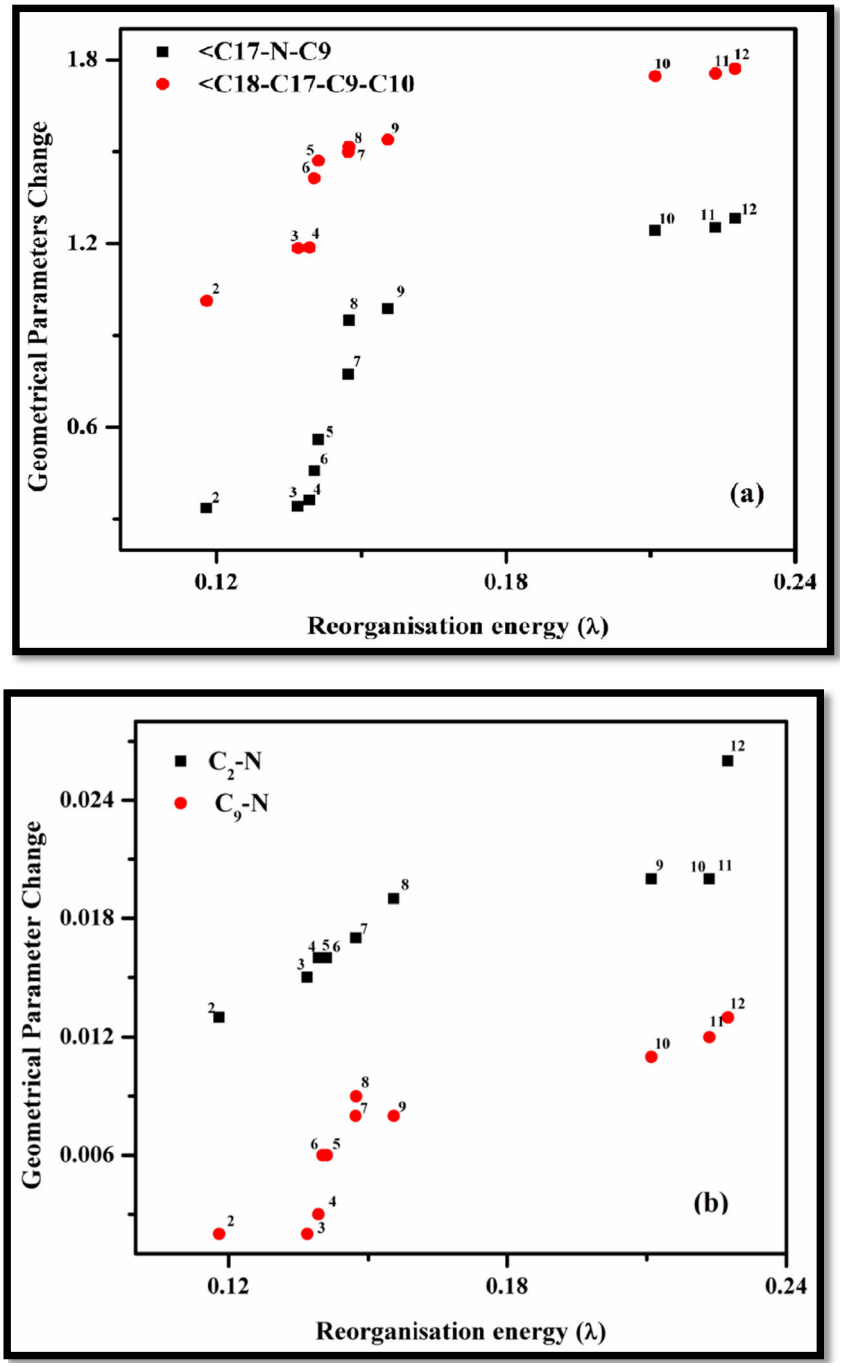

Fig. 3a,b Plot of reorganization energy with change in geometrical parameters. **a** Change in angle, **b** change in bond length for a series of TAH derivatives

expansions. Polarizability and hyperpolarizability characterizes the response of systems in an applied field. TAH is a π-conjugated framework created by $p_z$orbitals of each sp^2 hybridized carbon. This π-network is delocalized in nature, resulting in high electronic polarizability and hyperpolarizability, and giving rise to the active NLO response characteristic of such molecular systems. From the Gaussian 03 output file using the x, y, z components of a derivative, we calculated the dipole moment (μ), polarizability (α) and hyperpolarizability (β) of the TAH derivatives using Eqs. 4–6. From Table 4, it can be seen that all the hyperpolarizability terms are affected significantly by the incorporation of electron-donating and electron-withdrawing substituents on TAH(**1**). The maximum value of the hyperpolarizability term was assigned to derivative TAH(**2**) and the minimum to TAH(**12**) containing strong electron-donating and strong electron-withdrawing substituents, respectively. Thus, these results suggest that the introduction of electron-donating substituents leads to more active NLO performance and a stronger response to external electric or optical fields. Vertical electronic excitation energies were carried out by

Table 3 HOMO, LUMO energies, ionization potentials (IP; eV) of the studied TAH derivatives calculated at B3PW91/6-311G (2d, 2p)++ level of theory

TAH	E(HOMO)	E(LUMO)	$\Delta E_{(H-L)}$	Δ(HOMO)[a]	Δ(LUMO)[b]	Ip(eV)[c]
1	−5.133	−2.174	2.959			7.646
2	−4.705	−2.130	2.575	0.428	0.044	6.858
3	−4.734	−1.975	2.759	0.399	0.199	7.173
4	−4.776	−1.930	2.847	0.357	0.244	7.456
5	−4.760	−1.929	2.831	0.373	0.245	7.536
6	−4.784	−1.928	2.856	0.349	0.246	7.518
7	−5.355	−2.412	2.843	−0.222	−0.238	7.732
8	−5.395	−2.435	2.961	−0.262	−0.261	7.713
9	−5.447	−2.452	2.996	−0.314	−0.278	7.693
10	−5.494	−2.148	3.446	−0.361	0.026	7.816
11	−5.499	−2.113	3.485	−0.366	0.060	7.980
12	−5.538	−2.104	3.434	−0.405	0.070	8.088

[a] $\Delta(HOMO)=E(_{HOMO\ DMB\ derivative}) - E(HOMO_{DMB})$

[b] $\Delta(LUMO)=E(_{LUMO\ DMB\ derivative}) - E(HOMO_{DMB})$

[c] $Ip=E^{+}(G)^{0} - E^{0}(G)^{0}$

TD-DFT employing B3PW91/6-311++ G (2d,2p), performed for isolated molecules. According to the two level model of Oudar and Chelma [78], first hyperpolarizability is related to the low-lying CT transition on the basis of the complex sum over states (SOS) expression as:

$$\beta \propto \left(\mu_{ee} - \mu_{gg}\right) \frac{\mu_{ge}^2}{E_{ge}^2} \tag{8}$$

where (μ_{ee}− μ_{gg}) is the difference between the dipole moments of the *m*th excited state and ground state respectively, μ_{ge} is the transition dipole, and E_{ge} is the transition energy.

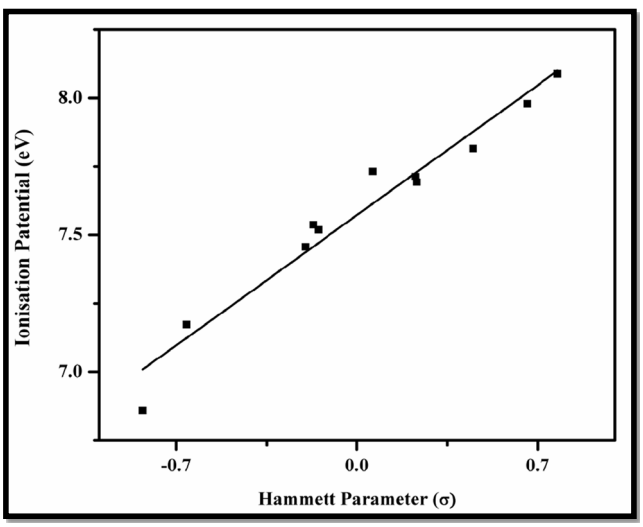

Fig. 4 Plot of Hammett parameter (σ) with ionization potential (IP; eV) for the series of studied TAH derivatives

According to this expression, the first hyperpolarizability (β) is proportional to the square of the transition dipole and is inversely proportional to the square of the transition energy. Thus, according to this model, the transition energy becomes the decisive factor for large β values. Therefore, materials with well-performing NLO properties should possess low-lying CT excited states with good oscillator strength [78]. It is clear from Table 4 that there is an enhancement of β values of TAH derivatives with increasing donor/acceptor abilities as compared to TAH(**1**), except for TAH derivatives **10,11** and **12**. According to Eq. 8, the value of β increases with increasing μ_{ge}^2 and decreasing E_{ge} values. In the case of TAH derivatives with electron-donating groups, the observed trend for μ_{ge}^2/E_{ge}^2 values is **2>3>4>6>5**, and the hyperpolarizability values increase in the order of **2>3>4>5>6**. On comparing the $-C(CH_3)_3$- and $-C_2H_5$-substituted derivatives (**4, 5**) with the methyl-substituted derivatives (**6**), it was found that (**6**) has a higher μ_{ge}^2 value than **5** and a lower value than **4**. However, the hyperpolarizability of both substituted molecules **4** and **5** is higher than that of the methyl substituted (**6**) derivative. Comparing the value of μ_{ge}^2/E_{ge}^2 of electron-releasing groups with those of electron-withdrawing groups, the former have comparably higher values than the latter. Thus, the contribution of the square form to the two-model dominates as the major effect on hyperpolarizability. The value of $\mu_{ge}^2/E_{ge}^2$for -floro substituted compound (**7**) is higher than the ethyl and methyl substituted derivatives (**5,6**); however, the hyperpolarizability of TAH (**5**) and TAH (**6**) is higher than that of the -floro substituted derivatives. Considering the two extremes of the series, i.e., the nitro derivative (strongest electron-withdrawing group) and dimethylamine derivative (strong electron-donating group), the values of β

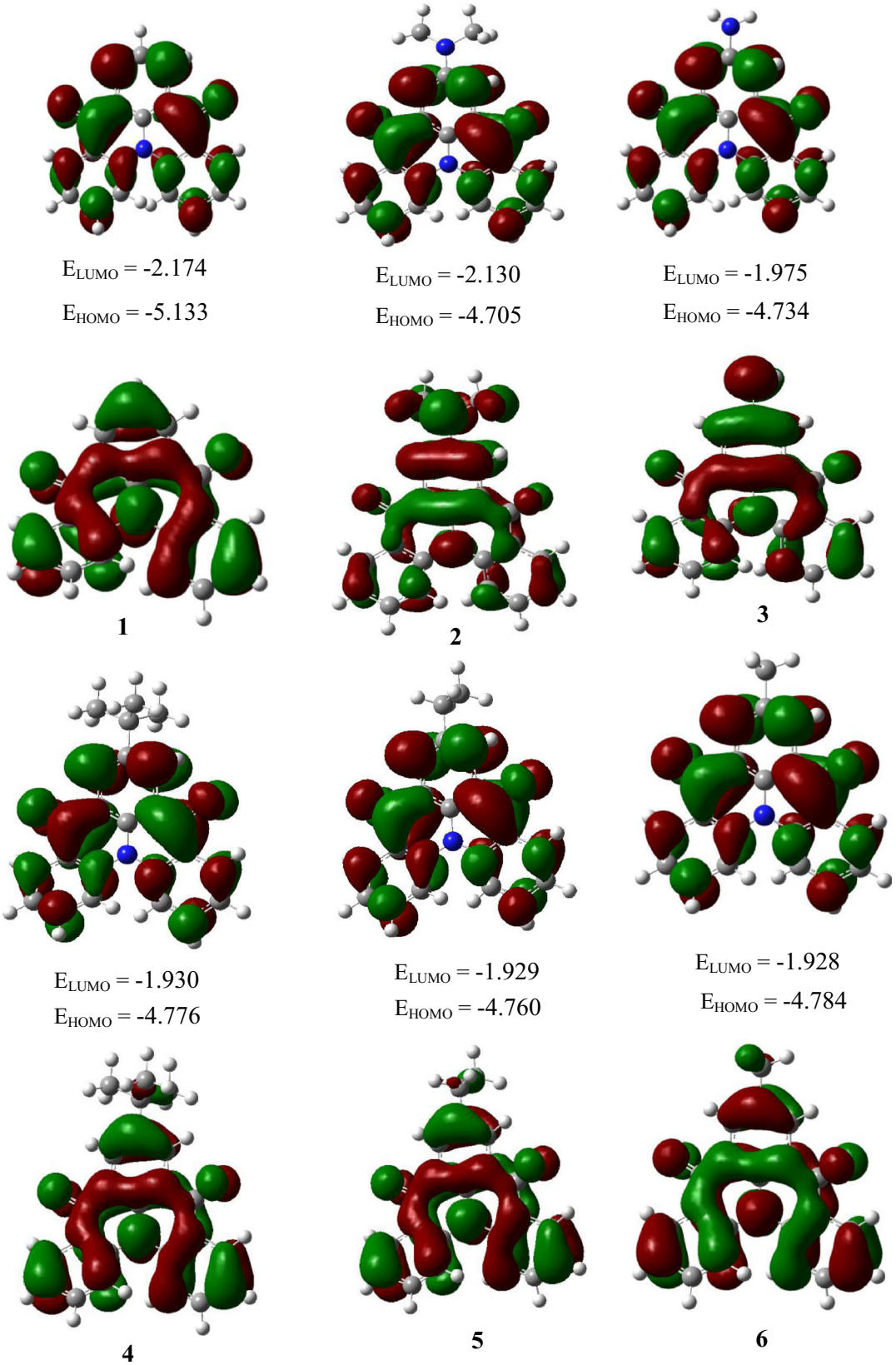

Fig. 5 Frontier molecular orbitals (FMO) of all the TAH derivatives

Fig. 5 (continued)

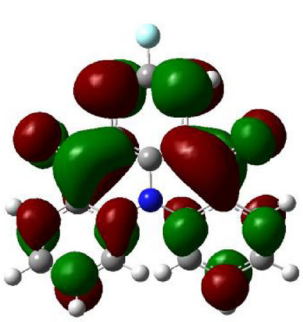

E_{LUMO} = -2.412
E_{HOMO} = -5.355

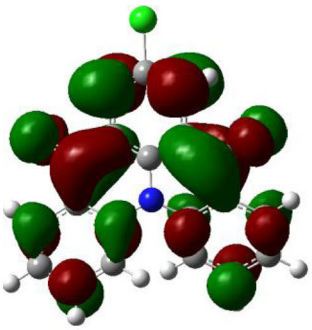

E_{LUMO} = -2.435
E_{HOMO} = -5.395

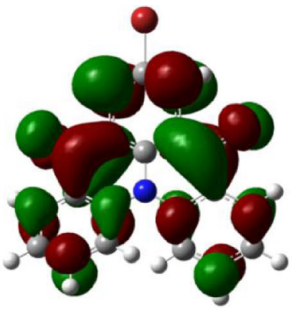

E_{LUMO} = -2.452
E_{HOMO} = -5.447

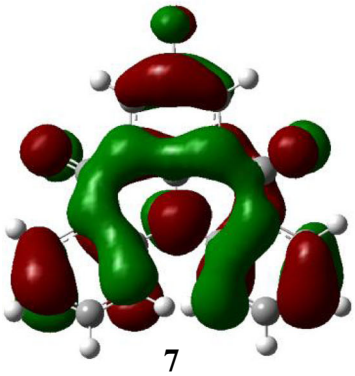

7

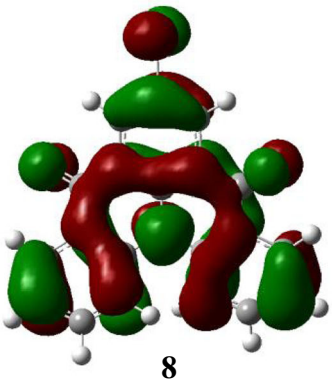

8

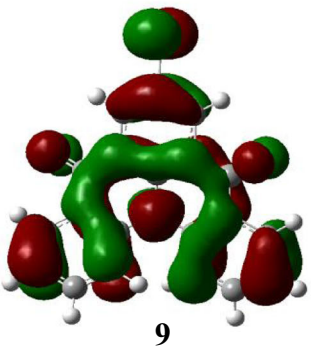

9

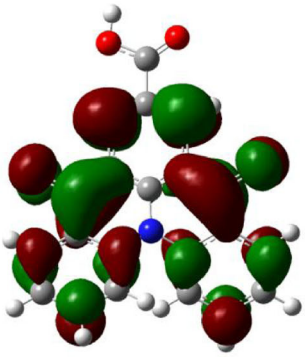

E_{LUMO} = -2.148
E_{HOMO} = -5.494

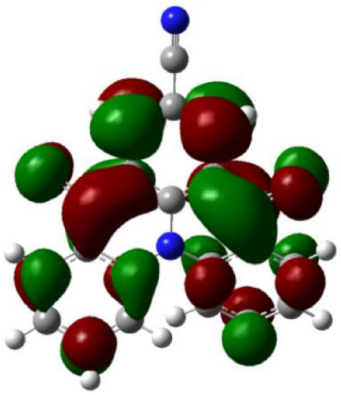

E_{LUMO} = -2.113
E_{HOMO} = -5.499

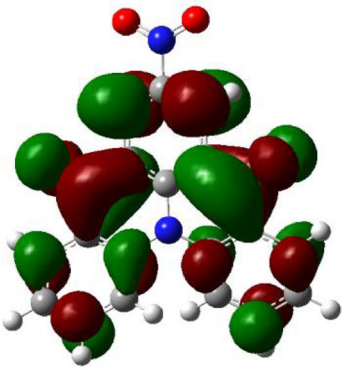

E_{LUMO} = -2.104
E_{HOMO} = -5.538

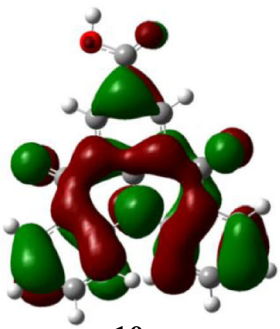

10

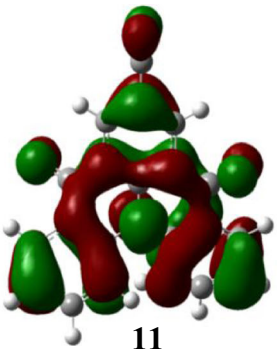

11

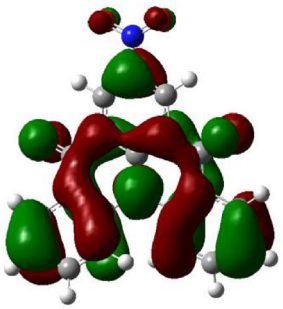

12

Table 4 Polarizability, hyperpolarizability and results of time-dependent density functional theory TD-DFT calculations at B3PW91/ 6-311G (2d, 2p)++ level of theory for the electronic transitions of all TAH derivatives

TAH	$\alpha(\times10^{-24}$esu)	$\beta(\times10^{-30}$esu)	λ_{max} (nm)	E_{ge}(eV)	μ_{ge}^2	μ_{ge}^2 / E_{ge}^2
1	47.127	1,205.388	403.10	3.449	0.490	0.041
2	56.907	20,434.375	506.20	2.546	2.554	0.394
3	56.386	15,018.051	487.04	2.742	2.205	0.293
4	53.467	9,564.149	452.15	2.814	2.164	0.238
5	53.223	8,671.068	433.31	2.918	2.036	0.224
6	52.559	5,597.251	420.99	2.932	2.062	0.227
7	52.278	2,413.296	420.62	2.945	2.011	0.232
8	51.218	1,386.146	425.87	2.953	1.855	0.213
9	50.068	1,215.181	429.13	2.948	1.764	0.203
10	48.799	924.454	411.66	3.076	1.563	0.165
11	48.242	897.895	410.80	3.001	1.530	0.170
12	47.417	840.543	408.22	3.037	1.263	0.137

are completely in accordance with the two model equation and depend upon the transition dipole and transition energy. The transition energy of TAH(**2**) is two-thirds that of TAH(**1**); however, the hyperpolarizability of TAH(**2**) is 20-fold compared to TAH(**1**). Thus, the value of hyperpolarizability, in addition to transition energy, also depends on the efficiency of electronic communication between the HOMO and LUMO involving intramolecular charge transfer. The maximum absorption band is composed primarily of electronic transition from the initial states, which are contributed by the HOMO and HOMO−1, to the final states, which are contributed mainly by the LUMO. The HOMO of the TAH derivatives are mainly π-type orbitals, hence they are sensitive to substituent properties. As the hydrogen in TAH(**1**) is replaced by dimethylamine, HOMO energy levels rise, resulting in a reduction in the energy gap. Thus, the electron density of the HOMO orbital of TAH(**2**) derivative favors CT to the LUMO orbital, confined toward the acceptor part of a molecule and results in an increase in the β value. Similarly, on comparing the halogen derivates of TAH, it was observed that, due to a reduction in the energy gap, the electron density shift results in intense CT compared to derivatives **10,11** and **12**, giving a high β value for TAH derivatives **7, 8** and **9** . The comparison discussed above reveals that, in addition to first transition energy, the intramolecular charge transfer in a noncentrosymmetric molecular environment is an important parameter for determining the value of hyperpolarizability.

Hammett parameter, bond length alternation and hyperpolarizabilities

We compared selected geometry parameters with values of β of TAH derivatives. In molecules with donating groups, the N–C_2 bond length was observed to be minimum for the dimethylamine derivative and maximum for the ethyl derivative and follows the order **2**<**3**<**4**<**5**=**6**, but the N–C_9 and N–C_{17} bond length decreases little from the dimethylamine derivative to the ethyl derivative and the hyperpolarizability follows the trend **2**>**3**>**4**>**5**>**6**. The increase in π-conjugation due to the + I (inductive) effect of electron-releasing groups causes an enhancement in the extent of resonance and results in geometrical modification of the derivative on account of attachment of electron-releasing substituents [57, 79–81]. Plots of hyperpolarizability of TAH derivatives as a function of σ (Fig. 6) reveal that hyperpolarizability of TAH derivatives with electron-releasing groups as well as electron-withdrawing groups decreases with increasing σ value expect in the case of TAH(**6**). The results fit a straight line with a correlation coefficient of 0.89 (or lower) for electron-releasing groups. On the other hand, a correlation coefficient of 0.91 (or higher) is observed for electron-withdrawing groups. According to Ulman, the

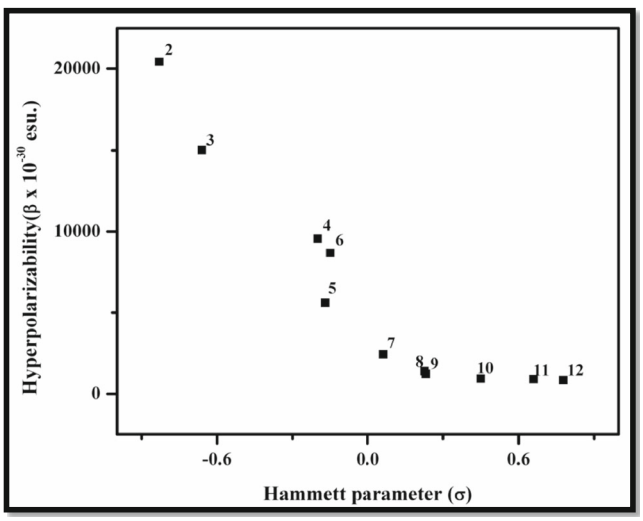

Fig. 6 Plot of hyperpolarizability against Hammett parameter of TAH derivatives with electron-donating and electron-withdrawing substituents

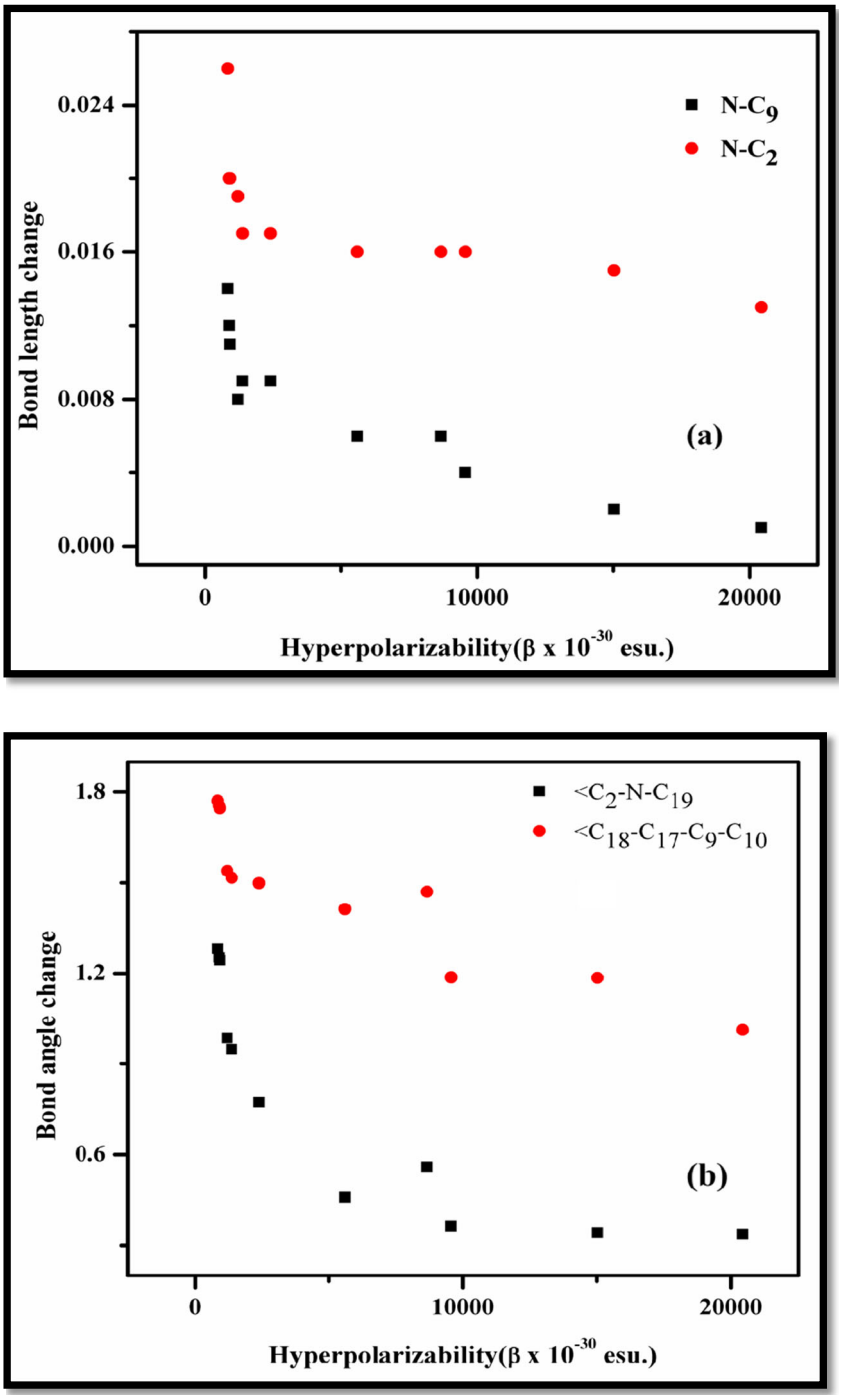

Fig. 7a,b Plot of hyperpolarizability against change in geometrical parameters for the series of TAH derivatives. **a** Change in bond length, **b** change in bond angle

inductive and resonance effects contribute to the Hammett substituent constant and both effects are important to the molecules [63, 64]. The donor group will easily push electrons towards the aromatic system and remain itself slightly electron deficient. This situation affects the magnitude of dipole moments as well as hyperpolarizability. Thus, the presence of different types of functional groups (electron-donating or electron-withdrawing abilities) affects the magnitude of hyperpolarizability of TAHs differently. To highlight the effect on hyperpolarizability of change in bond length and bond angle upon substitution, we plotted the hyperpolarizability of TAH derivatives versus changes in key bond lengths, bond angles and interplanar angles. The observed plots (Fig. 7a,b) reveal a close correlation between them for electron-releasing groups. In TAH derivatives with electron-releasing groups, the hyperpolarizability decreases in the order 20,434.375(**2**)> 15,018.051(**3**)>9,564.149(**4**) >8,671.068(**5**)>5,597.251(**6**) and the change in interplanar angle (<C_{18}–C_{17}–C_9–C_{10})

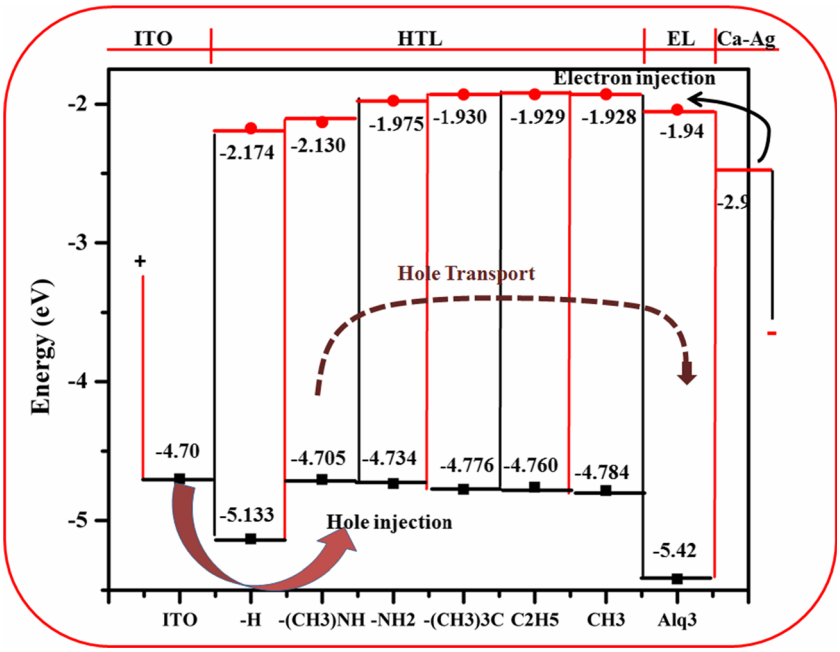

Fig. 8 Schematic diagram of a two-layered organic light emitting diode (OLED) device

follows the trend as 1.01<1.19=1.19<1.47>1.41. This indicates that the dimethylamino group is the strongest donor group and the methyl group is the weakest in this system, thus an increase in the strength of donor groups from methyl to dimethylamino have a pronounced impact on the hyperpolarizabilities. There is hardly any correlation between hyperpolarizabilities and the change in interplanar angle when the attached groups are electron withdrawing. In case of electron-withdrawing groups, the TAH derivative with the nitro group showed maximum change in geometrical parameters and hyperpolarizability, i.e., lower than that of fluorine TAH derivatives. Thus, we were able to correlate the key geometrical parameter BLA calculated by the Eq. 6 with hyperpolarizability. In TAH derivatives with electron-donating groups, the hyperpolarizability decreased in the order **2**>**3**>**4**>**5**>**6** and the BLA values followed the trend 0.369 (**2**) <0.371 (**3**) <0.375 (**4**)<0.381 (**5**) <0.382 (**6**). This shows that an increase in the strength of donor groups from methyl to dimethylamino has a clear impact on β values. However, there is only a weak correlation between hyperpolarizability and the BLA when the substituents are electron-withdrawing groups. TAH(**11**) and TAH(**12**) have the lowest β values, and highest BLA values, at 0.385 and 0.389, respectively, but in the case of **7**, **8**, and **9**, hyperpolarizability values decreases in the order **8**>**9**>**10**, while the BLA values do not differ much [0.385 (**7**) <0.386 (**8**)=0.386 (**9**)].This indicates that the withdrawing group has little effect on the BLA value and does not contribute to the change in hyperpolarizabilities. It can be concluded that changing the substituents for donor groups has a better effect on the BLA value and hyperpolarizability in this system.

From theory to efficiency

The theoretical data obtained in this study can be used to model OLEDs with optimum efficiency. Figure 8 shows a sketch of a typical single OLED based on indium tin oxide (ITO) as an anode, aluminum 8-hydroxy -quinolinate (Alq3) as an electron transporting/emitting layer (ETL/EL), a Ca-Ag cathode, and some of the studied TAH (with electron-donating groups) derivatives as the hole transporting layer (put together for comparison). The HOMO and LUMO levels for Alq3 were taken from experimental data. It has been shown elsewhere [18] that, in such devices, efficiency depends on the relative position of the HOMO–LUMO levels of the HTM viz-a viz the HOMO–LOMO levels of the ETL and the metal electrodes work function (Φ) (Φ for Ca=−2.9eV, Sm=−2.7 eV and Mg=−3.7eV), in addition to reorganization energy and IP.The efficiency of hole injection is controlled by the energy barrier between the work function of the ITO (Φ=−4.70) and the HOMO level of the HTM. From Fig. 8, we see that, for most of the TAH derivatives with electron donating groups as substituents, particularly **2** and **3,** the energy barrier is minimum. Further, a high energy barrier between EL/HTL to block migration of electrons from Alq3 to HTL, and a small energy barrier for hole transport on the HTL/ETL interface is required for high efficiency of the device. It is interesting to note that these essential requirements are met effectively by TAH derivatives **2**, **3**, **4**, **5**, **6** and **7** (see Fig. 8). Thus, on the basis of reorganization parameters, ionization energy and the

position of the frontier orbital energy levels, it is safe to conclude that the TAH derivatives with electron donating substituents perform best as HTMs as compared to parent TAH molecule.

Conclusions

The CT, NLO response and their relationship with structural modifications and energy levels of TAH derivatives were analyzed systematically using DFT at the B3PW91/ 6-311++ G(2d,2p) level of theory. The comparison of calculated geometrical parameters with corresponding experimental values showed reasonable agreement. The geometry of TAH (**1**) revealed the presence of three aryl rings linked through two bridged carbonyl groups and a planar central nitrogen atom. The gas phase optimizations revealed that the terminal rings are out of plane, with an interplanar angle of 46.19°. We found that the N–C_2 bond elongates with electron-donating substituents and shortens with electron-withdrawing substituents as compared to unsubstituted TAH(**1**), while N–C_9 and N–C_{17} bond lengths shorten with electron-donating substituents and elongate with electron withdrawing groups. The BLA studies revealed that BLA values increase upon substitution with electron-donating groups, indicating an enhancement in the degree of conjugation. We observed that reorganization energy values correlate well with changes in bond length, bond angle and interplanar angle. The strong electron-withdrawing substituents are responsible for large geometrical changes, while minimal changes in geometrical parameters, particular interplanar angles, were observed in the case of TAH derivatives with strong electron-donating substituents [–NH_2< –$N(CH_3)_2$]. Topological analysis of the HOMOs of neutral molecules revealed that these orbitals are concentrated mainly in the helicene backbone with a large contribution from fused phenyl rings, nitrogen atoms and carbonyl groups. However, the LUMO orbitals are invariably constituted by fused phenyl rings without any contribution from a central nitrogen atom. From the NLO study, we found that, in addition to transition energy, hyperpolarizability values also depended on the efficiency of electronic communication between the HOMO and LUMO involving intramolecular charge transfer. As the hydrogen in TAH(**1**) was replaced by the dimethylamine, the HOMO energy levels rose, resulting in a reduction in the energy gap. These results suggest that TAH derivatives with electron-donating substituents could be potential candidates for efficient charge carriers and can also be explored for use in productive NLO devices.

Acknowledgments We are thankful to the Head, Department of Chemistry, University of Kashmir, for providing the necessary laboratory facilities for carrying out this work. A.H.P. thanks the University Grants Commission (UGC), Government of India for research grant [F.No. 42-305/2013(SR)].

References

1. Gunter P (ed) (2000) Nonlinear effects and materials. Springer, Berlin
2. Karna SPJ (2000) PhysChemA 104:4671
3. Prasad PN, Williams DJ (1991) Introduction to nonlinear optical effects in molecules and polymers. Wiley, New York
4. Menard E, Meitl MA, Sun YG, Park JU, Shir DJL, Nam YS, Jeon S, Rogers JA (2007) Chem Rev 107:1117
5. Cheng YJ, Yang SH, Hsu CS (2009) Chem Rev 109:5868
6. Coropceanu V, Andre JM, Malagoli M, Bredas JL (2003) TheorChemAcc 110:59
7. Newman CR, Brisbie CD, da Silva Filho DA, Bredas JL, Ewbank PC, Mann KR (2004) Chem Mater 16:4436
8. Bunz UWF (2000) Chem Rev 100:1605
9. Wigglesworth TJ, Sud D, Norsten TB, Lekhi VS, Brand NR (2005) J Am ChemSoc 127:7272
10. Furche F, Ahlrichs R, Wachsmann C, Weber E, Sobanski A, Vogtle F, Grimme (2000) J Am Chem Soc 122:1717
11. Field JE, Hill TJ, Venkataraman D (2003) J Org Chem 68:6071
12. Maiorana S, Papagni A, Licandro E, Annunziata R, Paravidino P, Perdicchia D, Giannini C, Bencini M, Clays K, Persoons A (2003) Tetrahedron 59:6481
13. Lamanna G, Faggi C, Gasparrini F, Ciogli A, Villain C, Stephens PJ, Devlin FJ, Menichetti S (2008) ChemEur J 14:5747
14. Park JH, Yun C, Park MH, Do Y, Yoo S, Lee MH (2009) Macromolecules 42:6840
15. Xu Y, Zhang XY, Sugiyama H, Umano T, Osuga H, Tanaka K (2004) J Am ChemSoc 126:6566
16. Honzawa S, Okubo H, Anzai S, Yamaguchi M, Tsumoto K, Kumagai I (2002) Bioorg Med Chem 10:3213
17. Sato I, Yamashima R, Kadowaki K, Yamamoto J, Shibata T, Soai K (2001) AngewChemInt Ed 40:1096
18. Kuratsu M, Kozaki M, Okada K (2005) Angew Chem 117:4124
19. Kuratsu M, Kozaki M, Okada K (2004) Chem Lett 33:1174
20. Herse C, Bas D, Krebs FC, Burgi T, Weber J, Wesolowski T, Laursen BW, Lacour J (2003) Angew Chem 115:3270
21. Verbiest T, Kauranen M, Persoons A (1999) J Mater Chem 9:2005
22. Treboux G, Lapstum P, Wu Z, Silverbrook K (1999) ChemPhysLett 301:493
23. Manna AK, Pati SK (2009) Chem Asian J 4:855
24. Novoselov KS, Geim AK, Morozov SV, Zhang Y, Dubonos SV, Grigorieve IV, Firsov AA (2004) Science 306:666
25. Geim AK, Novoselov KS (2007) Nat Mater 6:183
26. Shinde PP, Kumar V (2011) Phys Rev B (Condens Matter Mater Phys) 84:125401
27. Franklin AD, Luisier M, Han SJ, Tulevski G, Breslin CM, Gignac L, Lundstrom MS, Haensch W (2012) Nano Lett 12:758
28. Hod O, Barone V, Scuseria GE (2008) Phys Rev B (Condens Matter Mater Phys) 277:035411
29. Potasz P, Guclu AD, Voznyy O, Folk JA, Hawrylak P (2011) Phys Rev B (Condens Matter Mater Phys) 83:174441
30. Barone V, Hod O, Scuseria GE (2006) Nano Lett 6:2748
31. Helveg S, Lauritsen JV, Lægsgaard E, Stensgaard I, Nørskov JK, Clausen B, Topsøe H, Besenbacher F (2000) Phys Rev Lett 84:951
32. Han WQ, Wu L, Zhu Y, Watanabe K, Taniguchi T (2008) Appl Phys Lett 93:223103
33. Lebegue S, Eriksson O (2009) Phys Rev B (Condens Matter Mater Phys) 79:115409
34. Andreas P, Humer M, Furchi MM, Bachmann D, Guider R, Fromherz T, Mueller T (2013) Nat Photonics 7:892

35. Eda G, Lin YY, Mattevi C (2010) Adv Mater 22:505
36. Li SS, Tu KH, Lin CC, Chen CW, Chhowalla M (2010) ACS Nano 4: 3169
37. Yang D, Zhou L, Chen L, Zhao B, Zhang J, Li (2012) Can ChemCommun 48:8078
38. Yamijala SRKCS, Pati SK (2013) J PhysChem C 117:3580
39. Yamijala SRKCS, Bandyopadhyay A, Pati SK (2013) arXiv: 1306.4873 [cond-mat.mtrl-sci]. doi: 10.1021/jp406344z
40. Shi H, Barnard AS A, Snook IK (2012) Nanoscale 4:6761
41. Lin BC, Cheng CP, Lao ZP (2003) J PhysChem A 107:5241
42. Cheng YC, Silbey RJ, da Siva Filho DA et al (2003) J ChemPhys 118:3764
43. Marcus RA (1957) J ChemPhys 26:867
44. Marcus RA (1957) J ChemPhys 26:872
45. Newman CR, Brisbie CA, da Silva Filho DA, Bredas JL, Ewbank PC, Mann KR (2004) Chem Mater 16:4436
46. Berlin YA, Hutchison GR, Rempala P, Ratner MA, Michl J (2003) J Phys Chem A 107:3970
47. Bredas JL, Beljonne D, Coropceanu V, Cornil J (2004) J Chem Rev 104:4971
48. Coropceanu V, Cornil J, Filho DAS, Olivier Y, Silbey R, Bredas JL (2007) Chem Rev 107:926
49. Marcus RA (1993) Rev Mod Phys 65:599
50. Nelsen SF, Blomgren FJ (2001) Org Chem 66:6551
51. Nelsen SF, Trieber DA, Ismagilov RF, Teki Y (2001) J Am Chem Soc 123:5684
52. Cheng LT, Tam W, Stevenson SH, Meredith GR, Rikken G, Marder SR SR (1991) J Phys Chem 95:10631
53. Clays K, Wostyn K, Persoons A, Maiorana S, Papagni A, Daul CA, Weber V (2003) Chem Phys Lett 372:438
54. Botek E, Spassova M, Champagne B, Asselberghs I, Persoons A, Clays K (2005) Chem Phys Lett 412:274
55. Lambert C, Noll G, Schelter J (2002) Nat Mat 1:69
56. Lakshmi S, Dutta S, Pati SK (2008) J Phys Chem C112:14718
57. Datta A, Pati SK (2006) ChemSoc Rev 35:1305
58. Spassova M, Asselberghs I, Verbiest T, Clays K, Botek E, Champagne B (2007) Chem Phys Lett 439:213
59. Pandith AH, Islam N, Syed ZF, Rehman S, Bandaru S, Anoop A (2011) Chem Phys Lett 516:199
60. Frisch MJ, Trucks GW, Schlegel HB et al (2004) GAUSSIAN 03 Revision B 03. Gaussian, Inc., Wallingford CT
61. Zhang R, Du B, Sun G, Sun Y (2010) Spectrochim Acta A 75:1115
62. Sundaraganesan N, Karpagam J, Sebastian S, Cornard JP (2009) Spectrochim Acta A 73:11
63. Islam N, Naiz S, Manzoor T, Pandith AH (2014) Spectrochim Acta A 131:461
64. Islam N, Pandith AH (2014) J Coord Chem. doi:10.1080/00958972.2014.961921
65. Perdew JP, Burke K, Wang Y (1996) Phys Rev B (Condensed Matter) 54:16533–16539
66. Binkley JS, Pople JA, Hehre WJ (1980) J Am Chem Soc 102:939
67. McLean AD, Chandler GS (1980) J Chem Phys 72:5639
68. Bauernschmitt R, Ahlrichs R (1996) Chem Phys Lett 256:454
69. Koch W, Holthausen MC (2000) A chemist's guide to density functional theory. Wiley-VCH, Weinheim
70. Viruela PM, Viruela R, Ort E, Bredas JL (1997) J Am Chem Soc 119: 1360
71. Viruela PM, Viruela R, Ort E (1998) Int J Quantum Chem 70:303
72. Karpfen A, Choi CH, Kertesz M (1997) J Phys Chem A 101:7426
73. Leffler JE, Grunwald E (1963) Rates and equilibria of organic reactions. Wiley, New York
74. Fu Y, Shen W, Li M (2008) Macromol Theory Simul 17:385
75. Cias P, Slugovc C, Gescheidt G (2011) J PhysChem A 115: 14519
76. Bandyopandhyay A, Yamijala SRKCS, Pati SK (2013) Phys Chem Chem Phys 15
77. Tachinaba Y, Haque SA, Mercer IP, Durrant JR, Klug DR (2000) J PhysChem B 104:1198
78. Oudar JL, Chemla DS (1977) J ChemPhys 66:2664
79. Persoons A (2011) Opt Mater Express 1:5
80. Ulman A (1988) J PhysChem 92:2385
81. Lewis GN (1923) Valence and structure of atoms and molecules. Chemical catalog, New York